Supporting Information

Ronceret et al. 10.1073/pnas.0906273106

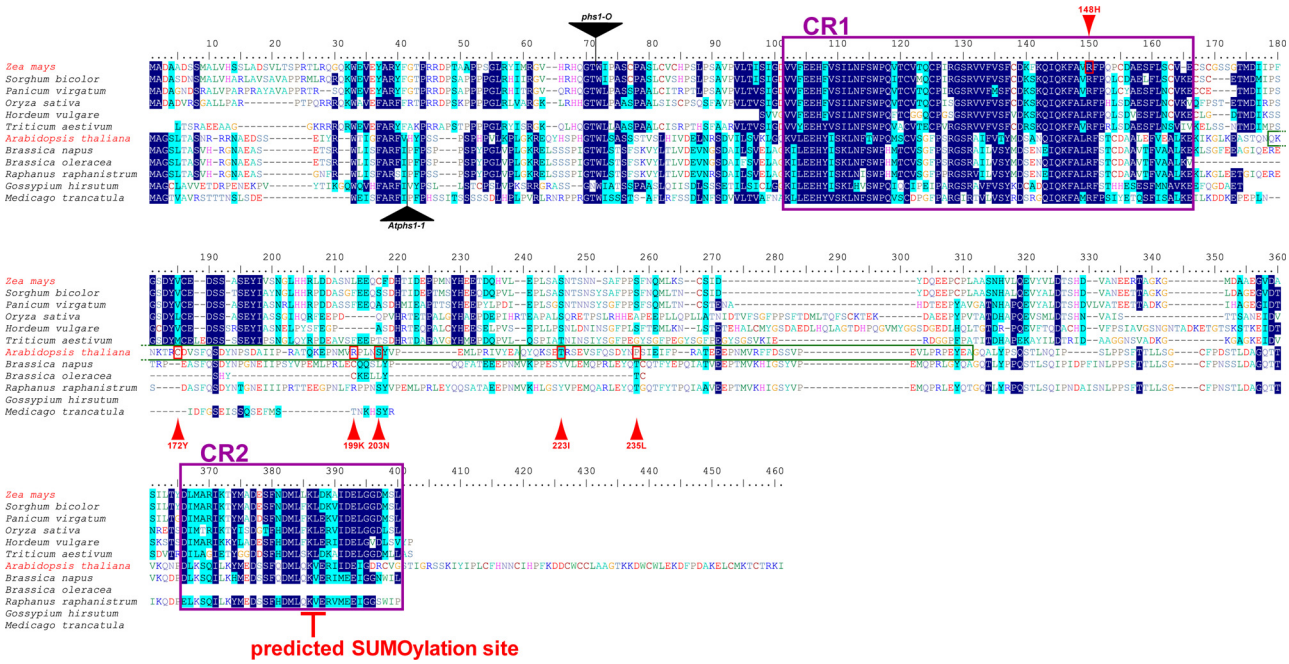

Fig. S1. Alignment of PHS1 homologs from monocot and dicot plants. Identities are shaded dark blue, similarities are shaded turquoise. Two conserved sequence regions, CR1 and CR2, are boxed in blue. Positions of insertional mutations in maize (*phs1-O*) and Arabidopsis (*Atphs1–1*) are marked with black triangles. Mutations created by TILLING are boxed in red and marked by red arrowheads, the positions of the mutated residues and the substituting amino acids are listed above or under the arrowheads. An internal duplication present in the Arabidopsis PHS1 sequence is boxed in green. For *Hordeum*, *Triticum*, *Brassica oleracea*, *Gossypium*, and *Medicago* only partial sequences were available.

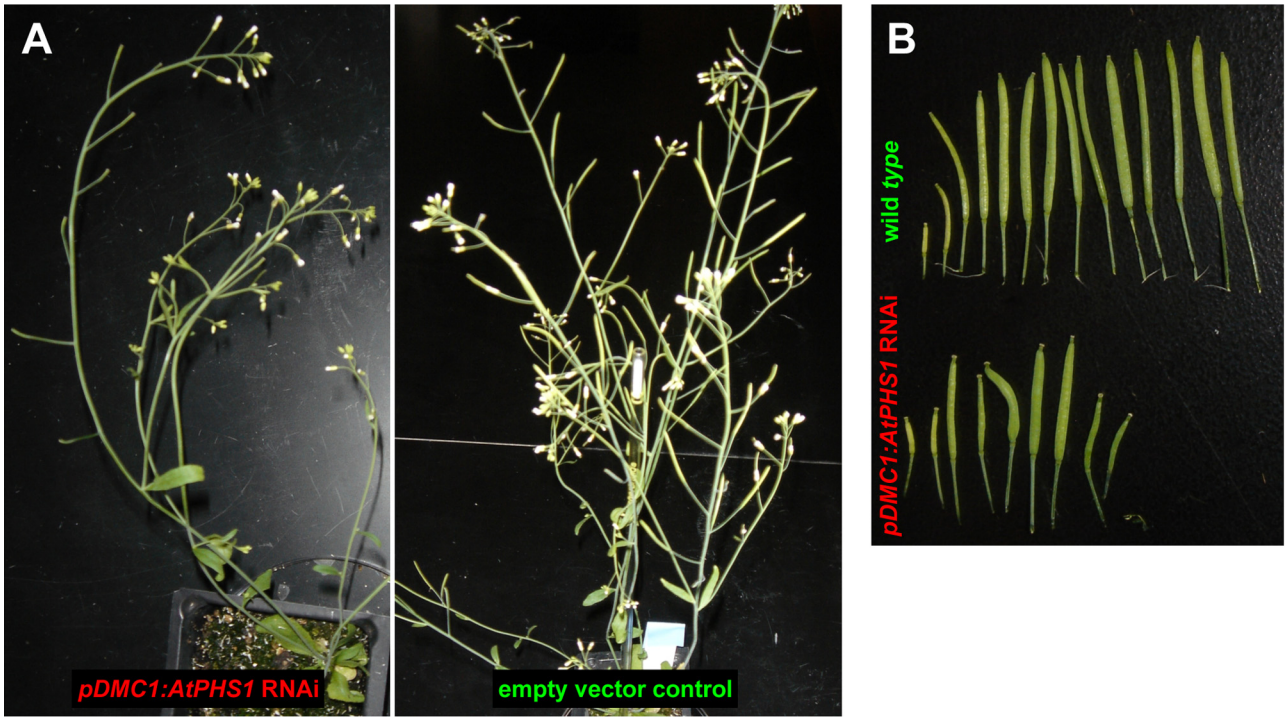

Fig. S2. Silencing of the *AtPHS1* gene using RNAi. (*A*) Comparison of phenotypes of transgenic plants carrying the *AtPHS1* RNAi silencing construct under the control of the *DMC1* promoter and an empty RNAi silencing construct. (*B*) Comparison of siliques collected from wild-type and transgenic *pDMC1:AtPHS1* RNAi plants. Plants expressing the RNAi construct produce small siliques that contain few seeds, indicating reduced fertility.

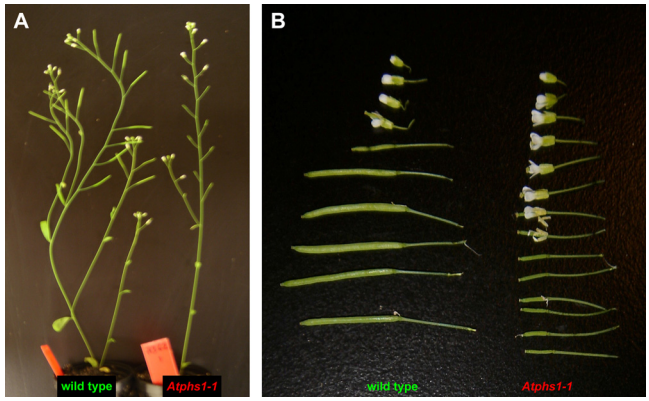

Fig. S3. The Arabidopsis *Atphs1–1* mutant. (*A*) Comparison of phenotypes of wild-type and *Atphs1–1* mutant plants. (*B*) Comparison of flowers and siliques collected from the main branch of single wild-type and *Atphs1–1* mutant plants. *Atphs1–1* mutants produce short siliques that contain few or no seeds.

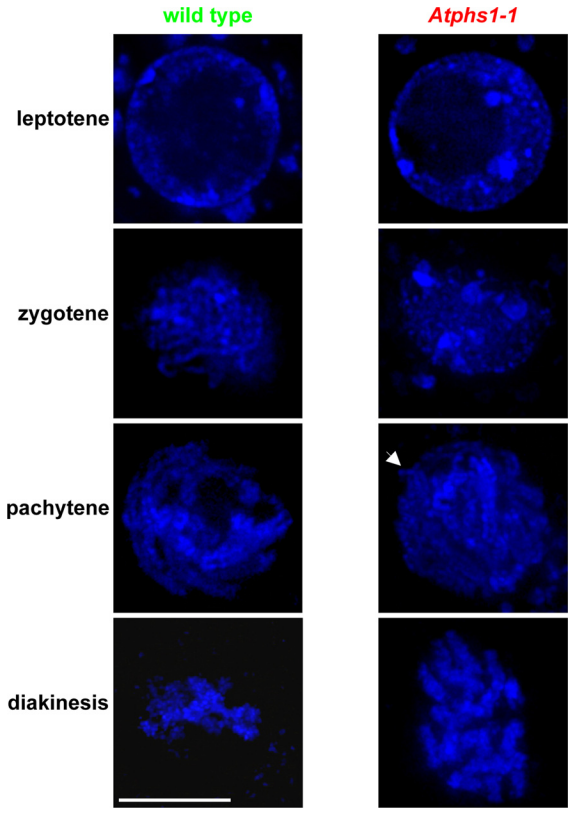

Fig. S4. Progression of meiosis in wild-type and *Atphs1–1* mutant meiocytes. Blue = chromatin. The white arrow marks misaligned chromosome ends in a bivalent. (Scale bar, 5 μm.)

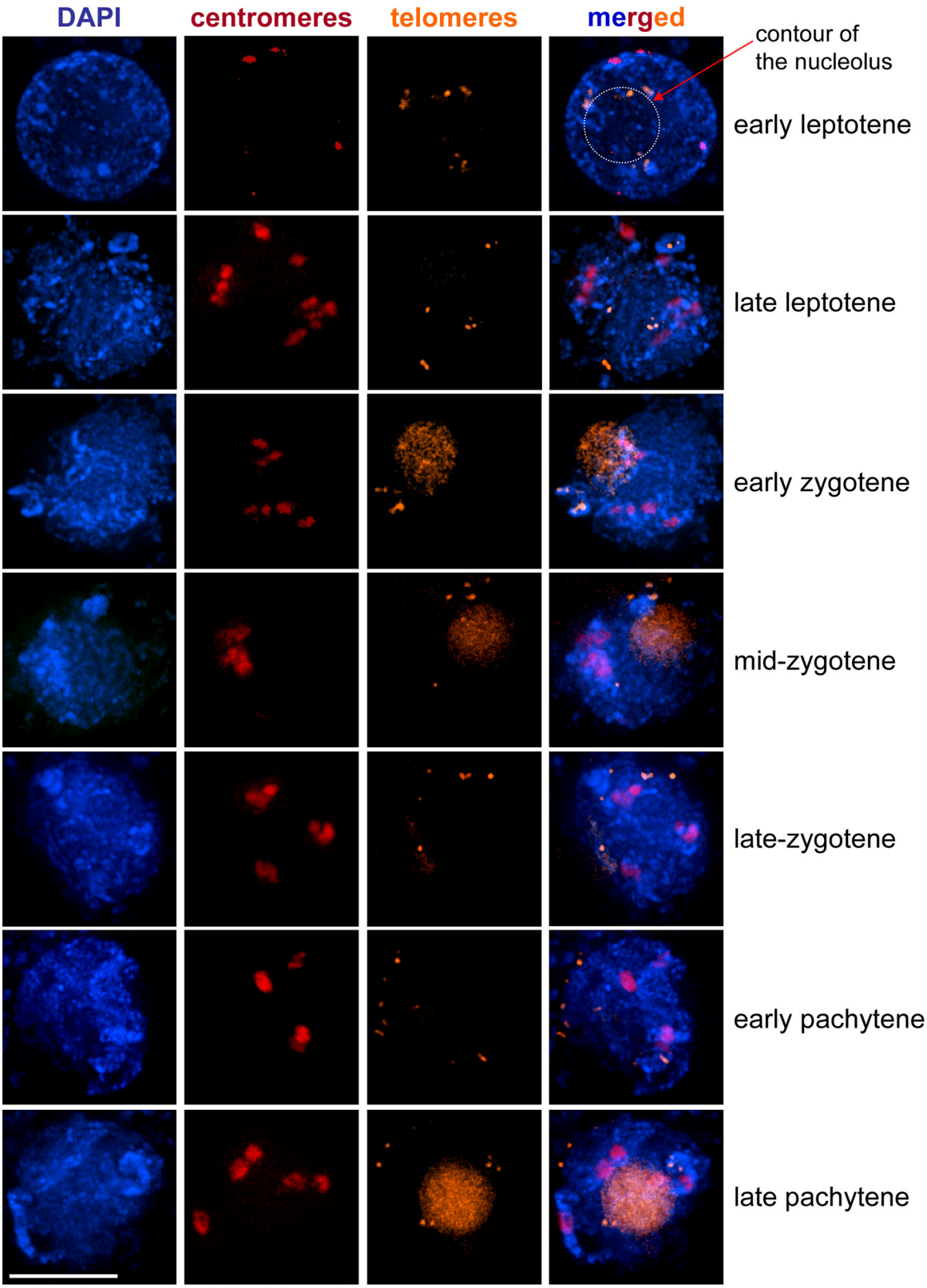

Fig. S5. Telomere and centromere behavior in the *Atphs1–1* mutant. Each image is a flat projection across the entire nucleus. The contour of the nucleolus is marked in the early leptotene image to show that telomeres cluster on the nucleolus. (Scale bar, 5 μm.)

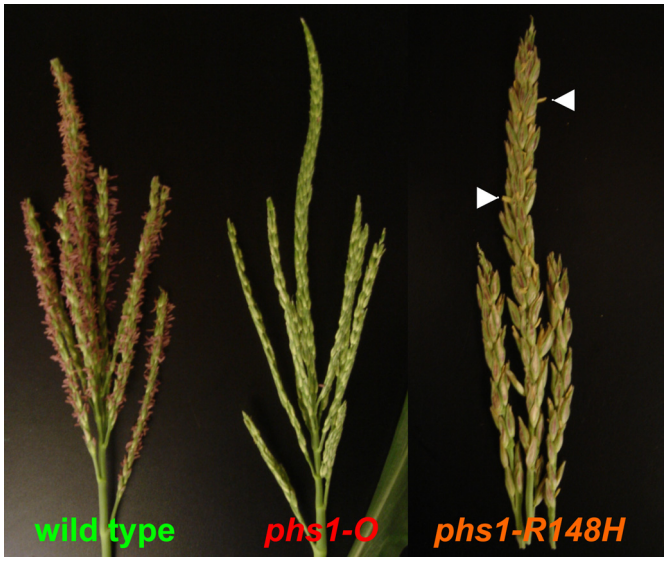

Fig. S6. Comparison of tassels from a wild-type, a *phs1-O* mutant and a *phs1-R148H* mutant plants. Anthers containing few pollen grains occasionally exert from flowers in *phs1-R148H* mutant (two examples are marked with white arrowheads) but very rarely in the null *phs1-O* mutant.

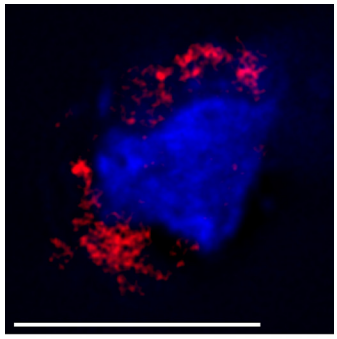

Fig. S7. Localization of the AtPHS1 protein in a zygotene meiocyte of the *spo11–1* mutant in Arabidopsis. Image represents a single optical section. (Scale bar, 5 μm.)

Table S1. Chromosome pairing in *Arabidopsis phs1* mutants

		Number of foci observed in pachytene				
Locus	*n*	2	3	4	5	6
5S rRNA loci						
Wild-type Ws ecotype	9	100.0%	0.0%	0.0%	—	—
pDMC1: AtPHS1 RNAi	15	20.0%	46.7%	33.3%	—	—
p35S: AtPHS1 RNAi	17	23.5%	35.3%	41.2%	—	—
Wild-type Nössen ecotype	7	—	100.0%	0.0%	0.0%	0.0%
Atphs1-1	14	—	21.4%	21.4%	28.6%	28.6%
25S rRNA loci*						
Wild type	12	100.0%	0.0%	0.0%	—	—
pDMC1: AtPHS1 RNAi	19	36.8%	26.3%	36.8%	—	—
Atphs1-1	16	25.0%	37.5%	37.5%	—	—

The *AtPHS1* RNAi lines are in the Ws ecotype, which harbors two pairs of 5S rRNA loci. The *Atphs1-1* mutant is in the Nössen ecotype, which has three pairs of 5S rRNA loci. Both ecotypes have two pairs of 25S rRNA loci.

*Although it has been reported that in FISH experiments using the chromosome spreading technique all 25S loci frequently cluster in meiotic prophase, we see this pattern very infrequently in 3-D microscopy. It is possible that the spreading technique causes the 25S loci, which are associated with the nucleolus, to cluster or that 3-D microscopy allows us to better separate closely located FISH signals.